

Technique Notes



Population cage recombination technique.

Bussel, Irvin. Department of Ecology and Evolutionary Biology, University of California, Irvine, CA, 92697; email: Ibussel@uci.edu

Fly scientists often separate a population from one cage into two in order to generate a larger egg-laying yield. This is done under the expectation that the resulting egg densities will be approximately around the expected standard density. However, under certain circumstances by separating the dense population into two cages, the resulting lower-density cages end up generating less than the original un-separated cage. Therefore, it is often desirable to recombine the cages in order to generate the expected density yield. However, due to the size of the cages, carbon dioxide is not a reasonable option to transfer flies from one cage to another.

The technique presented here requires that the plastic population cages have a durable cloth knotted on one end. In order to assure a successful manual transfer without loss of flies, the knots must be untied but the cloths must sustain a seal on the cages. Place some sort of food source into the cage you wish to become the primary combined cage. Pull a cloth from one of the cages over the other to form a tunnel. In the process, quickly remove the cloth over which you are forming a tunnel. This is very crucial because if the second cloth is left in the tunnel it will cause a blockade in the passage between both cages. At this point both cages should be connected by a single cloth that forms a connecting tunnel. Proceed to invert both cages vertically by holding one over the other to assure a clear downward path for the flies to follow. Most of the population should proceed into the cage with the food source. For the remaining ones that linger in the top secondary cage, shake the cage side to side to knock flies out of flight and down the tunnel. Once the primary cage contains the entire population, proceed to swiftly remove the cloth from the secondary cage and tie a knot to avoid escape. The primary cage should now have the entire population that therefore will allow for a greater egg-laying yield. This technique should prove useful for labs doing manual transfers without carbon dioxide or ether. It should also be important for those wishing to re-combine population cages effectively and efficiently.

Acknowledgments: I would like to thank Dr. Rose and Dr. Jafari for all their support and encouragement. I would also like to thank the students of the Rose Lab whose inquiries have made this possible.



A protocol for determining circulating hemocyte concentration of individual tumorous *Drosophila* larvae.

Sorrentino, Richard Paul,¹ and Robert A. Schulz. Department of Biochemistry and Molecular Biology, University of Texas M.D. Anderson Cancer Center, Unit 1000, 1515 Holcombe Boulevard, Houston, TX 77030; Tel. 713-834-6295; Fax 713-834-6291; ¹corresponding author (e-mail: rpsorren@mdanderson.org).

In order to determine the effects of mutations or other treatments on hematopoiesis in *Drosophila* larvae, it is advantageous to assess circulating hemocyte (blood cell) concentration (CHC). While hemacytometers have been used to assay CHC, there are nonetheless several disadvantages to using a hemacytometer: 1) samples must be examined immediately; 2) a maximum of two samples can be examined per visit to a microscope; 3) different hemocyte classes are sometimes difficult to distinguish in a brightfield microscope image of live hemocytes; 4) large aggregations of hemocytes (clumps), such as those found in larvae carrying mutations that induce the formation of hematopoietic tumors (e.g., *hopscotch*^{Tumorous-lethal}; Luo *et al.*, 1997), are not amenable to accurate counting. Herein we describe a simple and inexpensive method for determining CHC, by which we have obtained reliable and reproducible results (to be reported elsewhere). While this protocol can detect significant reductions (as compared to wild-type values) in CHC, there is obviously a lower limit to this sensitivity, and this protocol as described is not recommended for larvae that carry mutations that result in a severely reduced circulating hemocyte population. It also must be pointed out that this protocol does not examine the population of “sessile” hemocytes also found in *Drosophila* larvae.

Preparation of special fused tips

Prior to obtaining blood (hemolymph) samples from *Drosophila* larvae, special altered pipette tips (“fused tips”) must be prepared. The following supplies are necessary:

- plastic pipette tips, 200- μ l capacity (any supplier)
- scissors or straight razor blade
- Bunsen burner
- borosilicate glass capillary tubes (recommended product: item no. 1B100-4; World Precision Instruments, Sarasota, FL, USA)
- nail polish/enamel.

Using scissors or a razor blade, cut the smaller end of a number of pipette tips so that the bore of the resultant opening at the end of each tip is just large enough to accommodate a capillary tube. Borosilicate glass capillary tubes need not be more than a 3-4 cm long; longer capillary tubes can be broken in half by hand roughly at their midpoints (alternatively, a pipette puller can be used to make capillary tubes that have very fine points). Using one cut pipette tip and one capillary tube segment, insert the broken end of the tube (or the larger end of a pulled tube) into the cut smaller end of the pipette tip; briefly expose the end of the pipette tip to the open flame of a Bunsen burner. The plastic pipette tip should melt somewhat, allowing the glass capillary tube to be fused to the plastic pipette tip. Twisting the capillary tube while it is in contact with the melted plastic improves the final product. Set the fused tip aside to cool; repeat the procedure to produce as many fused tips as are needed. Once enough fused tips have been generated, airtight seals can be made by the application of nail polish/enamel to each joint; it is best to apply the nail polish to the entire circumference of the joint. Fused tips are ready to use when dry.

Obtaining hemolymph samples

In order to obtain hemolymph samples, the following items are required:

- dissecting microscope that provides underlighting
- glass microscope slides
- hemacytometer

very fine forceps, two pairs (recommended product: catalog no. 11254-20; Fine Science Tools, Foster City, CA, USA)
moist chamber that can accommodate a microscope slide
halocarbon oil (recommended product: halocarbon 27 oil; Halocarbon Products Corp., River Edge, NJ, USA; *n.b.*: any oil less dense than water will suffice)
one 25-mm Petri dish
2 μl and 20 μl pipettors
20-200 μl pipette tips
phosphate-buffered saline (PBS), working concentration
4% formaldehyde in PBS
4.17 ng/ μl Hoechst nuclear dye in PBS
fused plastic-glass tips (described above)
PAP pen (recommended product: catalog no. ACLMU12; Accurate Chemical and Scientific Corp., Westbury, NY, USA)

Glass microscope slides must be prepared in advance. For every ten larvae that you examine, you will need two slides: a "PBS slide" and a "sample slide." Clean each slide using 95% ethanol. Using a PAP pen, draw two rows of five circles on each slide; allow the slide to dry. On one slide ("PBS slide") place 10 μl of phosphate-buffered saline (PBS) into each circle, and place slide into a moist chamber. The "sample slide" does not receive any PBS and is kept in a dry covered container.

Fill the 25 mm Petri dish halfway with halocarbon oil. Attach a fused tip to a 20 μl pipettor; set pipettor to 10 μl . Attach a 2- or 10- μl -capacity (no greater) pipette tip to the 2 μl pipettor; set pipettor to 1 μl . Wash individual larvae twice in PBS and once in 95% ethanol (in order to remove any yeast from their surfaces) and place a larva onto a glass microscope slide that has been washed in 95% ethanol ("dissecting slide;" no PAP pen markings on this slide) onto the stage of a dissecting microscope; it is best to use underlighting in order to see hemolymph.

Open the larva using two pairs of very fine forceps. Hemolymph will spill out and collect around the larval carcass. Uncover the Petri dish and place it onto the microscope stage alongside of the slide. Using the fused tip, take up a small amount of halocarbon oil; quickly make sure that the seal of the fused tip is airtight by pressing down and up slightly on the pipettor piston while the fused tip is immersed in the oil (oil layer should move up and down within the tube; if this does not happen, quickly replace the fused tip with another and repeat test). Take up hemolymph pooled around larval carcass; make sure that no bubbles are present (*n.b.*: keep the hemolymph at the tip of the capillary tube; do not draw the hemolymph farther into the tube). Quickly return the fused tip to halocarbon oil and take up another small aliquot of oil. Cover the Petri dish and move it off of the microscope stage.

At this point, one should have a pure hemolymph sample trapped between two layers of halocarbon oil at the tip of the glass capillary tube. Remove the dissecting slide from the microscope stage. Place the hemacytometer onto the microscope stage and increase magnification to the maximum. Align the fused tip that has the hemolymph sample alongside of the hemacytometer grid; a large groove on either side of the grid will allow the fused tip to be held parallel to the grid at the same distance from the objective lens as the grid is. The menisci of the oil-hemolymph boundaries are concave with respect to the hemolymph sample; measure and record the height of the hemolymph column (the distance between the apices of the two menisci; estimates can be made to the nearest 0.05 mm). Remove the hemacytometer from the microscope stage. Recording the height of the hemolymph column must be done in such a manner as to allow one to match a later recorded value to a specific sample on a specific sample slide.

Remove the PBS slide from moist chamber and place onto microscope stage. Inject the oil and hemolymph into one PBS drop. Evenly distribute hemocytes in PBS drop by repeated suctioning using the pipettor. The oil will either float to the surface of the drop or form a droplet inside the PBS. Discard the fused tip. Using the 2 μl pipettor (set to 1 μl) take up 1 μl of diluted hemolymph; avoid taking up any oil droplets floating within the PBS. Return the PBS slide to the moist chamber. Transfer the prepared "sample slide" from its dry covered container onto the microscope stage. Apply the 1 μl diluted hemolymph sample to one PAP circle on the sample slide. Return the sample slide to the dry covered container.

This procedure can be repeated ten times per slide. Multiple larvae can be dissected on the same dissecting slide, as long as samples do not touch each other.

Allow all samples to dry thoroughly, then fix the samples by gently placing a drop of 4% formaldehyde (in PBS) onto each sample; samples should be fixed for 3 minutes. Remove 4% formaldehyde using a pipettor (taking care not to damage samples with pipette tip). Place one drop of Hoechst nuclear dye solution (4.17 ng/ μl in PBS) onto each sample. Incubate the samples for 5 minutes. Wash the samples twice with PBS, gently using a pipettor to apply and remove PBS to each individual sample (*n.b.* shortcuts such as dipping the entire slide into a solution or tilting the slide to allow the PBS to run off are not acceptable, as such manipulations allow for the mixing of samples). Cover the slide in 50% glycerol in PBS and a cover slip. Once one is proficient in this protocol, it is possible to obtain one slide of ten fixed, dyed, and covered samples in about twenty minutes. Prepared slides can be stored for later examination at 4°C for four weeks or more.

Calculation of CHC

In order to determine CHC for each sample, examine prepared sample slides on a fluorescent compound microscope with a filter appropriate for viewing Hoechst nuclear dye. For each sample, every hemocyte must be counted; the use of a hand counter is highly recommended. If desirable, different hemocyte classes can be noted. The volume of the original hemolymph sample in microliters (V_H) can be estimated as the volume of the cylindrical space taken up by the hemolymph within the capillary tube plus the volume of the biconcave ends: $V_H = \pi r^2 [h_1 + h_2 - (4/3) r]$, in which r = inner radius of capillary tube (mm); h_1 = height of the hemolymph column (mm); $h_2 = 2r$ (mm; h_2 = height of the column containing the meniscus, assuming each meniscus is a perfect hemisphere). The dilution factor is calculated as $DF = V_H / (V_H + 10 \mu\text{l})$. CHC for each larva (hemocytes/ μl) is then calculated as [(number of hemocytes in a 1 μl sample) / DF].

Statistical analysis

The distribution of wild-type CHC values does not conform to the normal distribution and is much better approximated by a log-normal (natural logarithm) distribution (Sorrentino *et al.*, 2004). Mean values and standard deviations of the natural logarithms (\ln) of individual raw CHC values can be obtained, allowing the comparison of means by Student's *t*-test. Logarithmic mean and standard deviation values can then be back-transformed as described in Limpert *et al.* (2001) in order to produce multiplicative mean and standard deviation values in concrete terms of hemocytes/ μl . As this protocol makes use of a dilution and an approximation of the volume of raw hemolymph samples, it is highly recommended that one make use of at least twenty individual hemolymph samples in order to obtain reliable conclusions in one's analyses.

References: Limpert, E., W.A. Stahel, and M. Abbot 2001, *BioScience* 51: 341-352; Luo, H., P. Rose, D. Barber, W.P. Hanratty, S. Lee, T.M. Roberts, A.D. D'Andrea, and C.R. Dearolf 1997,

Molec. Cell. Biol. 17(3): 1562-1571; Sorrentino, R.P., J.P. Melk, and S. Govind 2004, Genetics 166(3): 1343-1356.



Comparison of methods and body parts for estimation of hydrogen peroxide production by isolated mitochondria from *Drosophila simulans*.

Katewa, Subhash D., Richard G. Melvin, and J. William O. Ballard*

Ramaciotti Centre for Gene Function Analysis, School of Biotechnology and Biomolecular Sciences, University of New South Wales, Sydney 2052, Australia; *

Corresponding author. Tel.: + 61 2 9385 2021; fax: + 61 2 9385 1483; *E-mail* address: w.ballard@unsw.edu.au (JWO Ballard).

Abstract

Free-radicals such as superoxide and hydrogen peroxide contribute to a variety of pathophysiological conditions ranging from neurodegenerative diseases to aging. The goal of this study is to compare methods and body parts for estimating the rate of hydrogen peroxide produced by mitochondria isolated from *Drosophila simulans*. We compared the Amplex Red reagent based assay, with and without the addition of superoxide dismutase, with the *p*-hydroxyphenylacetic acid based assay method. All methods showed the same trend; however, the Amplex Red method plus superoxide dismutase was more sensitive especially when the rate of hydrogen peroxide production was low. We then compared hydrogen peroxide production from abdomen plus thorax with mitochondria extracted from thorax muscles only. Different body parts differentially estimated rates of hydrogen peroxide produced as organisms age. Future studies could compare the rate of age-dependent mitochondrial reactive oxygen species production from a multitude of tissues in flies with significantly different lifespan.

Introduction

Mitochondria are not only the cell's major metabolic energy suppliers, but are also the main intracellular source and target of reactive oxygen species and oxygen free-radicals generated by the respiratory chain complexes. In flies, respiratory chain complexes I and III are thought to be the major sites of oxygen free-radical production in the mitochondrion (Chen *et al.*, 2003; Miwa *et al.*, 2003). Complex I releases superoxide anions towards the matrix side whereas complex III releases superoxide on either side of the inner mitochondrial membrane. Measurement of the rate of superoxide formation from these sites in the intact mitochondria is difficult because it is (i) short lived, (ii) unable to cross the inner mitochondrial membrane, (iii) spontaneously dismutated to hydrogen peroxide (H₂O₂) by superoxide dismutase (SOD) present in the mitochondrial matrix, and (iv) invisible to detection reagents that do not enter the mitochondria.

A goal of this study is to compare methods for estimating the rate of H₂O₂ produced by mitochondria isolated from *Drosophila simulans*. These methods of measuring mitochondrial reactive oxygen species take advantage of the quantitative stoichiometric dismutation of superoxide to H₂O₂ and the ease with which H₂O₂ is able to permeate the mitochondrial membrane. Thus, the rate of H₂O₂ released from mitochondria reflects, but does not directly measure, the rate of intramitochondrial generation of superoxide. The released H₂O₂ is quantitated by a coupled reaction in which horseradish peroxidase is used to catalyze the oxidation of a dye, forming a fluorescent or a

light absorbent product in the presence of H_2O_2 . Therefore, the increase in fluorescence or absorbance is directly proportional to the amount of H_2O_2 generated in the mitochondria, and the rate of H_2O_2 generation can be measured by monitoring the rate of increase in fluorescence or absorbance.

The second goal of this study is to compare body parts for estimating the rate of H_2O_2 production with age. This study was considered important because there is conflicting data in the literature. Mitochondria extracted from whole flies show no increase in H_2O_2 production with age (Miwa *et al.*, 2004). In contrast, H_2O_2 released by mitochondria extracted from thoraces (Melvin and Ballard 2006; Ross, 2000; Sohal *et al.*, 1995; Sohal and Sohal, 1991) and head plus thoraces combined (Fridell *et al.*, 2005) increases with age in *Drosophila*.

Materials and Methods

Comparison of methods

For each method four replicate mitochondrial preparations extracted from thoraces of HW09 males were assayed at 11, 18 and 25 days (Melvin and Ballard, 2006). H_2O_2 production from complex I and from glycerol 3-phosphate dehydrogenase and complex III followed Katewa and Ballard (in press). For complex I, reactions contained 5mM proline and 5mM pyruvate as substrates and 2 μ M rotenone as a blocker. Only those preparations with a respiratory control ratio of 5 or more were included. Pyruvate and proline generate NADH in the citric acid cycle and electrons from NADH enter the electron transport chain at complex I. Rotenone blocks the flow of electrons from complex I to the next electron carrier in the chain, ubiquinone. For glycerol 3-phosphate dehydrogenase and complex III, H_2O_2 production was measured in reactions containing 5mM *sn*-glycerol 3-phosphate as substrate and 2 μ M rotenone as a blocker. In this assay rotenone prevented the back-cycling of electrons to complex I from ubiquinone and, therefore, H_2O_2 detected by the assay is believed to be produced from glycerol 3-phosphate dehydrogenase and complex III (Miwa *et al.*, 2003).

Spectrophotometrically, we assayed H_2O_2 production with Amplex Red and Amplex Red plus SOD (Molecular Probes, Eugene, OR) (Chen *et al.*, 2003). Fluorometrically, we tested the p-hydroxyphenylacetic acid (PHPA) method with added SOD (Hyslop and Sklar, 1984).

Amplex Red: Reaction of Amplex Red reagent with H_2O_2 in the presence of horseradish peroxidase produces the oxidation product, resorufin, which has an absorption maximum at 560 nm (Chen *et al.*, 2003). H_2O_2 production was measured as the increase in absorbance at 560 nm every 2 min for 1 hr at 25° C using a Molecular Devices, SpectraMax Plus spectrophotometer and SoftMAX Pro software (Molecular Devices Corp., Sunnyvale, CA). The initial linear phase of increase in absorbance at 560 nm was used to calculate the rate of H_2O_2 production per mg of mitochondrial protein. Each individual reaction volume was 100 μ l containing: 5 μ g of mitochondrial protein, respiration buffer (40 mM glycylglycine, 10 mM KH_2PO_4 , 5 mM $MgCl_2$, 120 mM KCl, 1.25 mg/ml fatty acid-free bovine serum albumin, pH 7.4), 100 μ M Amplex Red reagent, 0.1 U/ml horseradish peroxidase and electron transport complex specific substrates and inhibitors as described above.

Amplex Red plus SOD: A second set of Amplex Red reactions were prepared as described above with the addition of 30 U/ml SOD. Added SOD will dismutate superoxide released towards the inter-membrane space to H_2O_2 and is expected to estimate total H_2O_2 production. As such this method is expected to be a more accurate indicator of the total H_2O_2 production by intact mitochondria.

PHPA plus SOD: The 100- μ l reactions contained 5 μ g of mitochondrial protein, respiration buffer, 0.33M PHPA, 6 U/ml HRP, 30 U/ml SOD and electron transport complex specific substrates and inhibitors. Reactions were incubated at 25° C and fluorescence emission at 400 nm

(accumulation of (PHPA)₂) was measured every 2 min for 1 hr using a Molecular Devices, Gemini spectrofluorometer ($\lambda_{\text{excitation}} = 312 \text{ nm}$, $\lambda_{\text{emission}} = 400 \text{ nm}$) and SoftMAX Pro software. The initial linear phase of increase in fluorescence emission at 400 nm was used to calculate the rate of H₂O₂ production per mg of mitochondrial protein.

Comparison of body parts

We used the 'Amplex Red plus SOD' method to study whether the rate of mitochondrial H₂O₂ production differs at 11, 18 and 25 days in different body parts. For this study *D. simulans* males from Kenya were included. Mitochondria were isolated from abdomen plus thorax or thorax muscles only. Heads were removed from the abdomen plus thorax samples to prevent the red eye pigment from interfering with Amplex Red assays. Both heads and abdomens were removed in thorax only samples. H₂O₂ produced by complex III was assayed in reactions containing 5mM *sn*-glycerol 3-phosphate as substrate (Katewa and Ballard, in press).

Results

Comparison of methods

In all assay methods H₂O₂ production from complex I in HW09 mitochondria increased significantly over time (Figure 1.A). ANOVA shows that H₂O₂ production is affected by age ($F_{2, 18} = 43.84$, $p < 0.0001$), and by assay method ($F_{2, 18} = 5.77$, $p = 0.01$). There is no interaction between age and assay method ($F_{4, 18} = 0.32$, $p = 0.86$). The effect of assay method was due to a higher level of H₂O₂ detected by Amplex Red with added SOD than was detected by Amplex Red alone or by PHPA with added SOD (*post hoc* contrasts: $F_{1, 18} = 9.57$, $p = 0.006$, $F_{1, 18} = 7.62$, $p = 0.01$, respectively).

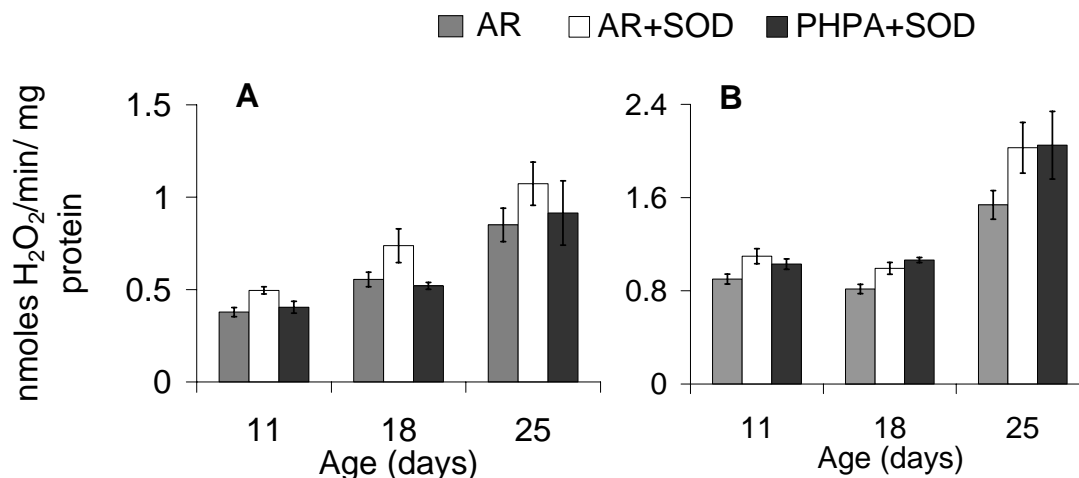


Figure 1. Rate of H₂O₂ production by mitochondria isolated from male *Drosophila simulans* (HW09) assayed at 11, 18, and 25 days after eclosion using three different assay methods. A. H₂O₂ produced from complex I. B. H₂O₂ produced from complex III. AR, Amplex red method; AR+SOD, Amplex red method with added superoxide dismutase (SOD); PHPA+SOD, *p*-hydroxyphenylacetic acid method with added SOD. The results are given as means of at least four independent mitochondrial extractions and the error bars indicate S.E.M.

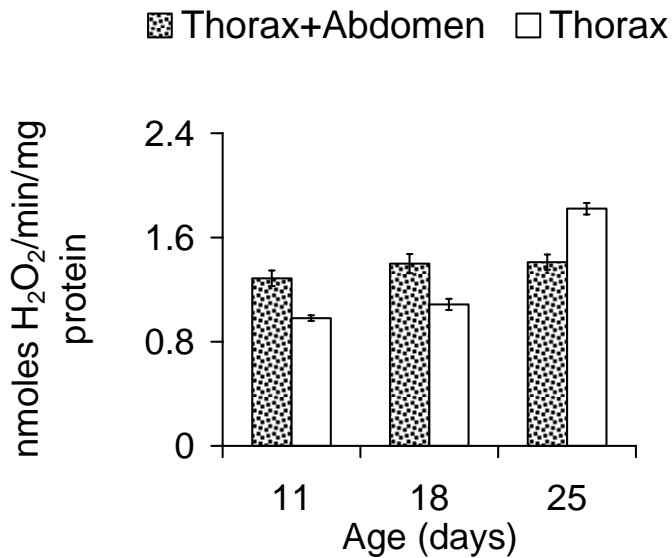


Figure 2. Rate of complex III H₂O₂ production by mitochondria isolated from different body parts of male *Drosophila simulans* (Kenya) flies. Mitochondria were isolated from abdomen plus thorax and thorax muscles only from 11, 18, and 25 day males. *sn*-glycerol 3-phosphate was used as the substrate. 30 U/ml superoxide dismutase was added in the assay. The results are given as means of at least four independent mitochondrial extractions and the error bars indicate S.E.M.

In all assay methods H₂O₂ production from complex III increased with age (Figure 1.B). ANOVA shows that H₂O₂ production is significantly affected by age ($F_{2, 18} = 68.24$, $p < 0.0001$) and by assay method ($F_{2, 18} = 7.02$, $p = 0.006$) but not their interaction ($F_{4, 18} = 1.17$, $p = 0.4$). The age effect was due to a significant increase in H₂O₂ production from 18 to 25 days after eclosion (*post hoc* contrasts: $F_{1, 18} = 106.99$, $p < 0.0001$). The effect of assay method resulted from the Amplex Red with no added SOD method detecting lower levels of H₂O₂ (*post hoc* contrasts: $F_{1, 18} = 10.58$, $p = 0.004$ and $F_{1, 18} = 10.46$, $p = 0.005$ for Amplex Red or PHPA with SOD, respectively).

Comparison of body parts

H₂O₂ production from complex III in Kenya flies showed distinctly different patterns (Figure 2). Two-way ANOVA suggests that H₂O₂ production is affected by age ($F_{2, 49} = 28.89$, $p < 0.0001$), not by body parts ($F_{2, 49} = 2.30$, $p = 0.14$), but there is strong interaction between age and body parts ($F_{2, 49} = 20.10$, $p < 0.0001$). One-way ANOVA further shows that H₂O₂ production increases with age in the thorax only samples ($F_{2, 17} = 147.95$, $p < 0.0001$) but not in thorax plus abdomen ($F_{2, 31} = 1.74$, $p < 0.20$) mitochondria.

Conclusions

All three methods showed an increase in H₂O₂ production with age in mitochondria isolated from thoraces. As such, all methods gave similar results and do not suggest any methodological biases. In our hands Amplex Red with SOD is likely the most accurate method when the concentration of H₂O₂ is low. In complex I measurements, the values obtained using the Amplex Red with SOD method were higher than those obtained using the Amplex Red without SOD or the PHPA with SOD methods (Figure 1A). Added SOD converted all superoxide to H₂O₂ and thus increased the levels of H₂O₂ measured. SOD was added to both the Amplex Red and the PHPA assays so the difference could be (i) Amplex Red was able to detect H₂O₂ at lower levels, (ii) resorufin formed was more stable than the fluorescent PHPA dimer, (PHPA)₂ at lower concentration, and/or (iii) the spectrophotometric method reader was more sensitive than the fluorometric reader. We have no direct evidence to support or refute any of these hypotheses but noted that the Amplex Red reagent was more light-stable than PHPA over the time course of the assay (data not shown).

Significantly different patterns were observed when we compared H₂O₂ production from mitochondria extracted from abdomen plus thorax compared with thorax alone. These data show that the rate of mitochondrial reactive oxygen species production in aging differs depending on the origin of the extracted mitochondria. H₂O₂ production from abdomen plus thorax is simpler and quicker to obtain as the thorax does not have to be removed. This may tend to give higher quality mitochondrial preparations. Further, it gives a more accurate estimate of the whole organism H₂O₂ production. Rates of H₂O₂ production from thoraces give a more accurate estimator of reactive oxygen species production from a single tissue but are more difficult to obtain. In this study we excluded all mitochondrial preparations with a respiratory control ratio of less than 5 when pyruvate and proline was the substrate. At this time it is not known whether there is any mechanistic relationship between rates of H₂O₂ production from any one tissue and any specific phenotype such as the rate of aging. Future studies could compare the rate of age-dependent mitochondrial ROS production from various tissues in flies with significantly different lifespan.

References: Chen, Q., E.J. Vazquez, S. Moghaddas, C.L. Hoppel, and E.J. Lesnefsky 2003, J. Biol. Chem. 278: 36027-36031; Fridell, Y.W., A. Sanchez-Blanco, B.A. Silvia, and S.L. Helfand 2005, Cell Metab. 1: 145-152; Hyslop, P., and L. Sklar 1984, Anal. Biochem. 141: 280-286; Katewa, S.D., and J.W.O. Ballard (In Press), Sympatric *Drosophila simulans* flies with distinct mtDNA show difference in mitochondrial respiration and electron transport. Insect Biochem. Mol. Biol.; Melvin, R.G., and J.W.O. Ballard 2006, Aging Cell. 5: 225-233; Miwa, S., K. Riyahi, L. Partridge, and M.D. Brand 2004, Ann. N. Y. Acad. Sci. 1019: 388-391; Miwa, S., J. St-Pierre, L. Partridge, and M.D. Brand 2003, Free. Radic. Biol. Med. 35: 938-948; Ross, R.E., 2000, J. Insect Physiol. 46: 1477-1480; Sohal, R.S., A. Agarwal, S. Agarwal, and W.C. Orr 1995, J. Biol. Chem. 270: 15671-15674; Sohal, R.S., and B.H. Sohal 1991, Mech. Ageing Dev. 57: 187-202.



Establishment of cell type specific Gal4-driver lines for the mesoderm of *Drosophila*.

Stute, Christiana^{1,2}, Dörthe Kesper^{1,3}, Anne Holz^{1,4}, Detlev Buttgerie¹, and Renate Renkawitz-Pohl^{1*}

¹Philipps-Universität Marburg, Fachbereich Biologie, Entwicklungsbiologie, Karl-von-Frisch-Str. 8, 35043 Marburg, Germany; ²present address: Max-Planck-Institut für Molekulare Physiologie, Abteilung II, Systemische Zellbiologie, Otto-Hahn-Str. 11, 44227 Dortmund, Germany; ³present address: Zentrum für medizinische Biotechnologie, Universität Duisburg-Essen, Entwicklungsbiologie I, Universitätsstr. 2, 45117 Essen, Germany; ⁴present address: Institut für Allgemeine und Spezielle Zoologie, Allgemeine Zoologie und Entwicklungsbiologie, Justus-Liebig-Universität Giessen, Stephanstrasse 24, 35390 Giessen, Germany. *Correspondence to: Renate Renkawitz-Pohl, renkawit@staff.uni-marburg.de

Introduction

During the development of the *Drosophila* somatic and visceral musculature, two different cell types, the founder cells and the fusion competent myoblasts (FCM), fuse with each other to form the multinucleate myotubes. In the case of the somatic musculature, this is a two-step process, in which a founder cell first fuses with one or two FCMs to form a muscle precursor. In a second wave of fusion, additional FCMs are recruited to reach the final muscle size. During the last years several genes were identified that are specifically expressed in one of the two cell types (reviewed in Taylor,

2003; Chen and Olson, 2004; Abmayr *et al.*, 2005). Several driverlines are published that drive expression in the entire mesoderm (*e.g.*, *24B-Gal4*, Brand and Perrimon, 1993; *Mef2-Gal4*, Ranganayakulu *et al.*, 1996; *twist-Gal4*, Baylies and Bate, 1996) or in subsets of the mesoderm, *e.g.*, the visceral mesoderm (*bap-Gal4*, Zaffran *et al.*, 2001). Nevertheless, so far only one cell type specific driverline for these different cell types has been published. This driverline, called *rP298-Gal4* (Menon and Chia, 2001), drives expression in the somatic and visceral founder cells from the determined founder cells and the first wave of fusion onwards. Up to now no driverline that drives expression in the FCMs or specifically in the founder and precursor cells of the somatic mesoderm has been published. Therefore we decided to analyse the promoter-region of *sticks and stones (sns)* (Bour *et al.*, 2000) to search for regions that drive expression in the FCMs of the visceral and somatic mesoderm. The genomic fragment was cloned into a Gal4-vector and injected into flies. The same was done for the 2 kb region upstream of *rolling pebbles7 (rols7)* to establish a driver line for the somatic founder cells.

Experimental Procedure

Generation of the Gal4-transformation vector and cloning of the sns-promoter region: To establish a driverline for the FCMs we excised the *lacZ* gene from pCHAB Δ Sal (Thummel *et al.*, 1988), with *Bam* HI and *Xba* I and replaced it by *Gal4* from pGATB (Brand and Perrimon, 1993) (pCHAB-Gal4). Next we amplified the 5' upstream region of *sns* with PCR using the oligonucleotides

GCCATTGGGCTGGCTGGTTCCTTG and GCTTGCAGAAGTGTGGGTGAACGG

and cloned the PCR fragment into TOPO-TA (Invitrogen). After sequencing, the insert was excised, cloned into the *Not* I site from pCHAB-Gal4 and checked for orientation (*sns-Gal4*).

Drosophila strains: *sns-lacZ* (reportergene construct expressing *lacZ* in the FCMs of the somatic and visceral mesoderm, this work), *sns-Gal4* (Gal4-driverline for the FCMs of the visceral and somatic mesoderm, this work), *Rols7-Gal4* (Gal4-driverline for the founder cells of the somatic mesoderm, this work), *UAS-Rols300-myc* (first 300 amino acids of Rols7 with a myc tag cloned into pUAST, Nina Kreisköther and Renate Renkawitz-Pohl unpublished). At least 3 independent flylines for each construct were established and analysed.

Antibodies and immunostaining: Immunostaining was performed as described before (Knirr *et al.*, 1999, Klapper *et al.*, 2002). We used anti- β -Galactosidase antibodies from Biotrend (dilution 1:2500, made in rabbit), anti-Myc antibodies from Cell signalling (dilution 1:1000, made in mouse), and Cy2 and Cy3 labelled secondary antibodies from Dianova (dilution 1:100).

Results and Discussion

Establishing a Gal4 driver line for the FCMs of the visceral and somatic mesoderm: *Sns* is expressed specifically in the FCMs of the visceral and somatic mesoderm from stage 11 onwards. Embryos carrying *lacZ* under the control of the 4.5 kb region upstream of the ATG of *sns (sns-lacZ)* reproduce the expression pattern observed for *Sns* (Figure 1 and Bour *et al.*, 2000). Namely the expression starts in stage 11 in two bands in the mesoderm (Figure 1 A). After fusion has occurred, *lacZ* expression can be detected in all developing muscles in the visceral and somatic mesoderm (Figure 1 B, C). Further there is an additional staining in the mesoderm of the gonads where *Sns* normally is not expressed (Figure 1 D).

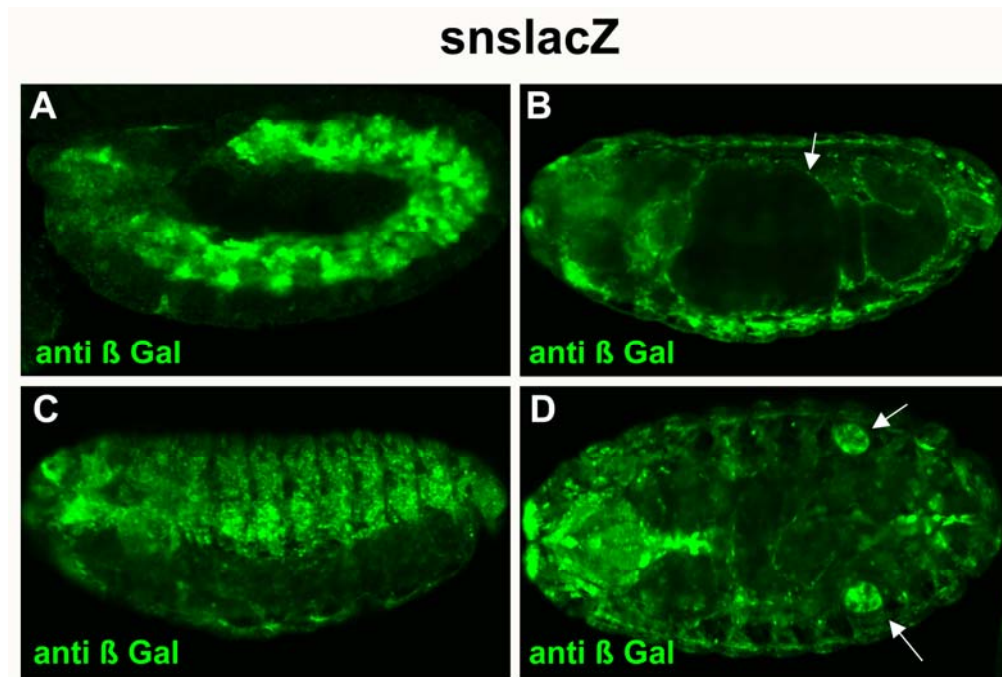


Figure 1. The *sns-lacZ* flies show expression in the FCMs of the visceral and somatic mesoderm from stage 11 onwards. Anti-β-Galactosidase staining on embryos carrying the *sns-lacZ* construct. A: In stage 11 expression can be found in the FCMs of the visceral and somatic mesoderm. B, C: Later on in stage 15 *lacZ* is expressed in the visceral (arrow in B) and somatic musculature. D: An additional staining can be observed in the mesoderm of the gonads in stage 17 (arrows in D).

We cloned the 4.5 kb fragment also into the pCHAB-Gal4 vector, established transgenic flies and crossed the resulting fly lines with *UAS-lacZ* (data not shown) and a fly strain that contains the first 300 amino acids of Rols with a myc-tag under the control of the *UAS*-element (*UAS-Rols300-myc*, Nina Kreisköther and Renate Renkawitz-Pohl, unpublished) to analyse the expression pattern (Figure 2). The expression of the *UAS-Rols300-myc* construct does not cause a phenotype. In both cases the expression of the reporter protein is detected later in comparison to the *sns-lacZ* lines. Initially in stage 11 the expression can only be observed in some cells of the mesoderm (Figure 2 A, B, arrow in C). These cells never express the founder cell marker *rP298-lacZ* (arrowhead in Figure 2 C, Nose *et al.*, 1998) at the same time, but are always adjacent to the founder cells, which makes it very likely that they are indeed FCMs. In stage 12 the number of FCMs showing reporter gene expression greatly increases. Later on most of the multinucleate muscles of the somatic (Figure 2 E) and visceral mesoderm (Figure 2 D) are marked by the reporter protein expression. Only some somatic muscles are not labelled (arrow in Figure 2 F). Therefore, it seems as if in stage 11, when the *sns* expression in the wild-type starts, the *sns*-Gal4 driver initiates expression of the reporter genes in only a subset of FCMs. This may be due to low levels of Gal4 unable to activate the reporter. At the end of embryogenesis most muscles are marked by the reporter protein. The driver does not initiate gene expression in all FCMs but in a great proportion of it. The unstained muscles vary from segment to segment, which is in good agreement with the assumption that the FCMs are not

subdivided into groups in which for example *sns* expression is initiated at different time points and thereby determines them to fuse with certain founder cells.

snsGal4>>UAS-Rols300-myc

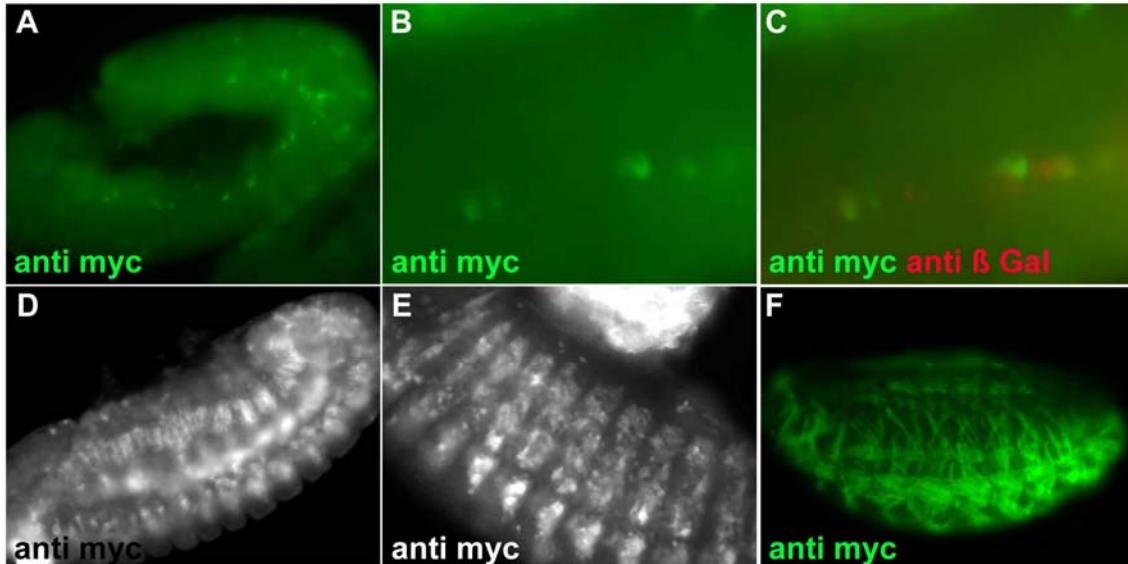


Figure 2. The expression of the reporter protein in the *sns*-Gal4 line is delayed in comparison to the *sns*-*lacZ* line. A-C: in stage 11 embryos the reporter protein expression is only initiated in a subset of cells by the *sns*-Gal4 driver (arrow in C). These cells are always adjacent to the *rP298-lacZ* positive founder cells (arrowhead, red in C). D-F: Later most somatic (E) and visceral (D) muscles express the reporter protein. The arrow in F indicates muscles that do not express the reporter protein.

Rols7Gal4 >> UAS-Rols300-myc

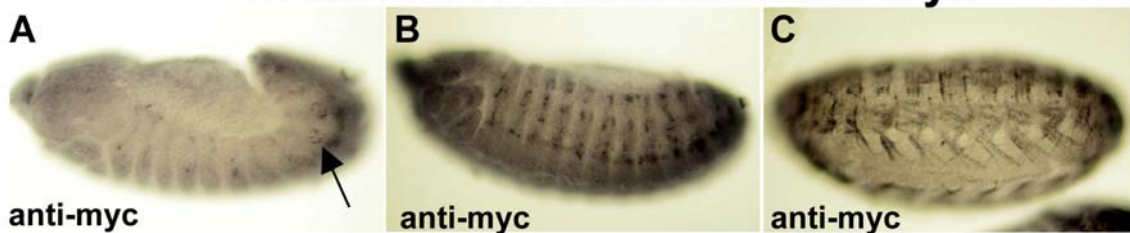


Figure 3. *Rols7*-Gal4 drives expression in the somatic mesoderm from stage 12 onwards. A: The expression of the reporter protein can first be observed in some cells of the somatic mesoderm of stage 12 embryos. B: During development the number of cells expressing the reporter protein increases. C: At the end of embryogenesis in stage 17 all muscles express the reporter construct.

Gal4-driverline for the somatic founder and precursor cells: The *rols* gene encodes for two transcripts, *rols6* and *rols7*. While Rols6 is expressed in the endoderm and the Malpighian tubules, Rols7 is expressed in the somatic, visceral and pharyngeal mesoderm. In the somatic mesoderm Rols7 expression is restricted to the founder and precursor cells (Rau *et al.*, 2001; Pütz *et al.*, 2005).

To obtain a driver line specifically for the founder cells of the somatic mesoderm, we cloned the 2 kb upstream of the *rols7* transcription start, which reproduces the full *rols7* expression pattern in the somatic mesoderm (Kesper *et al.*, in preparation) into the pCHABGal4 vector (*Rols7-Gal4*). After crossing this driver with *UAS-Rols300-myc* flies, we could observe expression of the Myc-tagged protein in the somatic mesoderm (Figure 3 A) from stage 12 onwards till the end of embryogenesis (Figure 3 B and C). When a *UAS-Rols7* construct is expressed under the control of this driver, it is able to partially rescue the fusion phenotype of *rols*-deficient embryos (data not shown).

Again in the *Rols7-Gal4* driverline the onset of expression of the reporter protein seems to be later in comparison to the *lacZ* construct (Kesper *et al.*, in preparation) and is only initiated in a subset of the precursor cells at the beginning, but later detectable in all precursors and muscles. This delay is probably due to the fact, that first the Gal4 has to be synthesised which then has to enter the nucleus of the cell and initiate the transcription of the reporter gene.

References: Abmayr, S.M., L. Balagopalan, B.J. Galetta, and S.J. Hong 2005, In: *Comprehensive Molecular Insect Science* Vol. 2. Oxford, Elsevier Ltd. p. 1-45; Baylies, M.K., and M. Bate 1996, *Science* 272: 1481-1484; Bour, B.A., M. Chakravarti, J.M. West, and S.M. Abmayr 2000, *Genes Dev.* 14: 1498-1511; Brand, A.H., and N. Perrimon 1993, *Development* 118: 401-415; Menon, S., and W. Chia 2001, *Developmental Cell.* 1: 691-703; Chen, E.H., and E.N. Olson 2004, *Trends Cell Biol.* 14: 452-460; Klapper, R., C. Stute, O. Schomaker, T. Strasser, W. Janning, R. Renkawitz-Pohl, and A. Holz 2002, *Mech Dev.* 110: 85-96; Knirr, S., N. Azpiazu, and M. Frasch 1999, *Development* 126: 4525-4535; Nose, A., T. Isshiki, and M. Takeichi 1998, *Development* 125: 215-223; Pütz, M., D.A. Kesper, D. Buttgerit, and R. Renkawitz-Pohl 2005, *Mech Dev.* 122: 1206-1217; Ranganayakulu, G., R.A. Schulz, and E.N. Olson 1996, *Dev Biol.* 176: 143-148; Rau, A., D. Buttgerit, A. Holz, R. Fetter, S.K. Doberstein, A. Paululat, N. Staudt, J. Skeath, A.M. Michelson, and R. Renkawitz-Pohl 2001, *Development.* 128: 5061-5073; Taylor, M.V., 2003, *Curr Biol.* 13: 964-966; Thummel, C.S., A.M. Boulet, and H.D. Lipshitz 1988, *Gene* 74: 445-456; Zaffran, S., A. Kuchler, H.H. Lee, and M. Frasch 2001, *Genes Dev.* 15: 2900-2915.



Direct Visualization of GFP-Fusion Proteins on Polytene Chromosomes.

DiMario, Pat*, Raphyel Rosby, and Zhengfang Cui. Louisiana State University, Department of Biological Sciences, Baton Rouge, LA 70803. *Corresponding author: Pat DiMario: pdimari@lsu.edu, 225-578-1512.

The following is a quick and easy protocol for localizing GFP-tagged proteins directly on the polytene chromosomes of third instar larvae. Briefly, salivary glands are fixed in formaldehyde, washed, soaked in 50% glycerol for a few minutes, and then finally squashed in 50% glycerol to spread the polytene chromosomes. We believe the glycerol mimics the viscosity of the nucleus to help chromosomes spread and to preserve their morphology. Since there is no acid fixation in this technique, GFP signals are well preserved. This technique may also offer an alternative fixation method for immuno-localizations using antibodies that fail to recognize irreparably damaged chromosomal proteins in conventional acid-fixed polytene chromosome preparations.

Microscope slide preparation: Microscope slides were prepared as described by Gall *et al.* (1991):

1) Wash standard microscope slides by bare hand (or with gloves that are free of talcum powder) in a working dilution of Linbro 7× Cleaning Solution. Rinse the slides using glass carriers that hold ~20

slides when you zig-zag them. Rinse with tap water for 30 min and then with several changes of distilled water.

2) Without allowing the slides to dry, dip each rack of slides into 5× subbing solution for 5 min.

5× subbing solution is:

250 ml of distilled water.

Add 1.25 g of gelatin (Knox gelatin from the grocery store is fine).

Microwave to dissolve.

Allow the solution to cool.

Add 0.125 g of Chrome Alum (Chromium potassium sulfate).

We add sodium azide to a final concentration of 0.04% to prevent mold growth on the protein-coated slides during prolonged storage.

3) After the 5 min soak in subbing solution, lean the racks to allow them to drain as much as possible, but then use a pipet whisker tip connected to a sink aspirator to remove excess subbing solution from between the slides. Otherwise, the slides stick together as they dry. Allow the slides to dry overnight, and then store them in a dust free slide box.

Polytene Chromosome Preparation: We perform the following procedures at room temperature using three-well glass dissection dishes.

1) Dissect third instar salivary glands directly into a formaldehyde solution.

We use Brower's Fixation Buffer (see Blair, 2000) which is:

0.15 M Pipes

3 mM MgSO₄

1.5 mM EGTA

1.5% NP40

Adjust the pH to 6.9.

Although it turns a bit cloudy, we store this solution at room temperature.

Just before use, add formaldehyde to a final concentration of 2%. We usually use commercial 37% formaldehyde, but freshly prepared paraformaldehyde should give better results.

Dissect the salivary glands directly into the formaldehyde solution. Fix the glands for 2-3 minutes. During this time clean off excess fat body as best you can. Final formaldehyde concentrations and fixation times have not been rigidly optimized, but we suspect chromosomes do not spread well if they are over-fixed.

2) Transfer the glands to 1 × PBS containing 0.1% Triton X-100 for another 2-3 minutes.

3) Transfer the glands to 50% glycerol (made with only distilled water). Allow the glands to soak for about 5 minutes. Longer incubations do not seem to help that much.

4) Transfer the glands to 13 micro liters of 50% glycerol on a subbed microscope slide (see above). Cover with a 22 × 22 mm cover slip (siliconized cover slips would be better, but we manage with cover slips taken directly from the box). Tap and squash as you see fit. Decent chromosomes are usually found on the periphery of the tissue debris field.

GFP-tagged proteins can be visualized and photographed at this point. We use phase contrast microscopy to capture the banding patterns.

Subsequent immuno-staining: Submerge a slide in liquid nitrogen for a few seconds until bubbling stops, withdraw the slide and quickly pop off the cover slip using a razor blade. Immediately submerge the still-frozen slide into $1 \times$ PBS. We store the slides in PBS until we accumulate enough preps for immuno-localizations.

Perform immuno-localizations by standard techniques. For example:

- 1) Block the chromosomes for 30 min with $1 \times$ PBS that contains 3% BSA, 0.1% NP-40, and 0.1% Tween 20.
- 2) Probe with a primary antibody diluted with the same blocking solution.
- 3) Wash several times with $1 \times$ PBS containing 0.1% Triton X-100.
- 4) Re-probe with a rhodamine-coupled secondary antibody diluted with blocking solution.
- 5) Wash as in step 3, store in $1 \times$ PBS with 0.04% azide.

Figure 1 shows an example of GFP and antibody co-localization on the polytene chromosomes. The GFP signal diminished only slightly after freezing and antibody labeling.

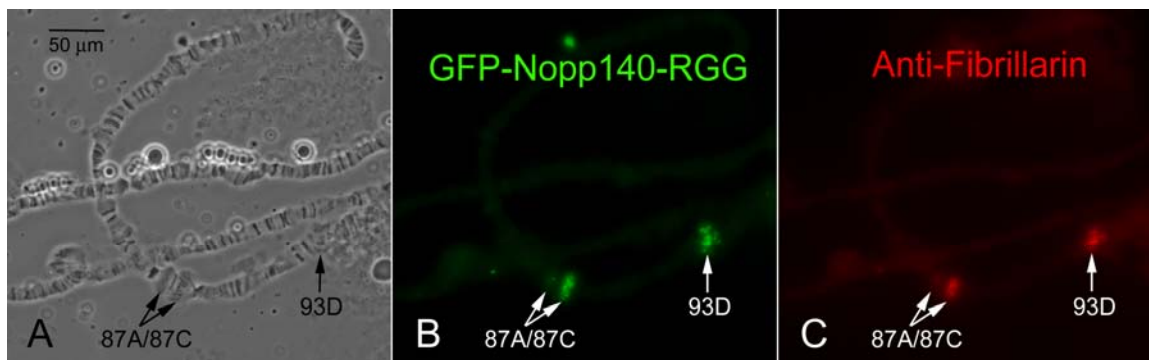


Figure 1. Third instar larvae transgenic for *Hsp70-GFP-Nopp140-RGG* (see McCain, *et al.*, 2006) were heat shocked for 1 hour at 37° C. Salivary glands were dissected 30 minutes into heat shock recovery, and the chromosomes were prepared as described above. Phase contrast images (A) and GFP-Nopp140-RGG localizations (B) were recorded immediately. The preparations were then frozen in liquid nitrogen and processed for immuno-fluorescence microscopy using mouse anti-fibrillarín, mAb 72B9, followed by a rhodamine-conjugated secondary antibody (C).

Results and Discussion

The polytene chromosome technique described above was developed to pursue an interesting but still preliminary observation, namely: Nopp140-RGG is normally a nucleolar protein that can

associate with certain heat shock transcripts. Nopp140-RGG has a carboxy terminal domain rich in RGG tri-peptide motifs. Such domains are common in RNA-binding proteins, including fibrillarin. By alternative splicing, *Drosophila* actually expresses two isoforms of Nopp140, Nopp140-RGG and Nopp140-True which is the *true* homologue to vertebrate Nopp140 (see Waggenger and DiMario, 2002). Both Nopp140 isoforms and fibrillarin localize to *Drosophila* nucleoli (McCain, *et al.*, 2006). Interestingly, GFP-Nopp140-RGG and apparently fibrillarin (see below) localized to the 87C and 93D heat shock loci of polytene chromosomes. GFP-Nopp140-True failed to do so, despite the fact that it and GFP-Nopp140-RGG localized to the giant nucleoli in these salivary gland cells (not shown here but see McCain, *et al.*, 2006).

Mouse mAb 72B9 labels fibrillarin which is well conserved in metazoans; mAb 72B9 labels *Drosophila* nucleoli quite well (see McCain, *et al.*, 2006). Although 72B9 failed to detect Nopp140-RGG by Western blot, we can not completely rule out the possibility that the antibody labels Nopp140-RGG on the chromosomes or in nucleoli.

Although intriguing, the localization of Nopp140-RGG to heat shock loci is not totally surprising since several heterogeneous nuclear RNA binding proteins with similar RGG motifs are known to interact with the non-translated hsr-omega transcript produced at 93D (Prasanth, *et al.*, 2000). Using the spreading technique described here we hope to further determine the specificity of interactions between various RGG-containing proteins and transcripts produced at the heat shock loci.

Acknowledgments: This work was supported by the National Science Foundation (grant MCB-0234245).

References: Blair, S., 2000, In: *Drosophila Protocols*. (Sullivan, W., M. Ashburner, and R.S. Hawley, Eds.). Cold Spring Harbor Laboratory Press, Cold Spring Harbor. pp. 159-173; Gall, J.G., C. Murphy, H.G. Callan, and Z. Wu 1991, *Methods Cell Biol.* 36: 149-166; McCain, J., L. Danzy, A. Hamdi, O. Dellafosse, and P. DiMario 2006, *Cell Tissue Res.* 323: 105-115; Prasanth, K.V., T.K. Rajendra, A.K. Lal, and S.C. Lakotia 2000, *J. Cell Sci.* 113: 3485-3497; Waggenger, J.M., and P.J. DiMario 2002, *Mol. Biol. Cell* 13: 362-381.



Protocol for the detection and analysis of cell death in the adult *Drosophila* brain.

Mitchell, Kevin J., and Brian E. Staveley. Department of Biology, Memorial University of Newfoundland, St. John's, Newfoundland & Labrador, Canada, A1B 3X9; telephone (709) 737-4317; telefax (709) 737-3018; Corresponding Author: Dr.

Brian E. Staveley; e-mail address: bestave@mun.ca

Introduction

Many neurodegenerative diseases, including Parkinson's disease, Alzheimer's disease, and Huntington's disease, are associated with the accumulation of toxic, aggregation-prone proteins (reviewed in Taylor *et al.*, 2002; Petrucelli and Dawson, 2004; Bodner *et al.*, 2006). Protein accumulation in neuronal cells, particularly in the endoplasmic reticulum (ER), results in stress and is suspected to trigger cell death and neurodegeneration (Lihong *et al.*, 2005; Ferreira *et al.*, 2006). The expression high levels of the yeast transcriptional factor GAL4 in *Drosophila melanogaster* results in increased apoptosis, a reduced life span, and reduced motor control (Haywood *et al.*, 2002; Kramer and Staveley, 2003). A protocol to remove the adult *Drosophila* brain quickly and analyze it for

increased levels of apoptosis may prove to be useful in the study of human neurodegenerative diseases in *Drosophila melanogaster* models.

***Drosophila* Strains and Culture**

Flies were raised on standard cornmeal/yeast/molasses/agar medium at 25°C in plastic vials. The *OrR*, *w*; *UAS-p35*, and *w*; *UAS-lacZ* stocks were obtained from the Bloomington *Drosophila* Stock Center. The *UAS-p35* chromosome has been re-balanced over *TM6C*, *Sb Tb e* in our laboratory. The *w*; *TH-GAL4* flies were generously provided by Serge Birman of the Developmental Biology Institute of Marseilles. The *w*¹¹¹⁸ flies were a gift from Howard Lipshitz of the University of Toronto. Non-*GAL4* controls were the progeny of *OrR* females and *w*¹¹¹⁸ males. The *w*; *TH-GAL4* flies are taken from the true-breeding stock. The *w*; *TH-GAL4/UAS-lacZ* and *w*; *TH-GAL4/UAS-p35* are the progeny of *w*; *TH-GAL4* females and the appropriate (*w*; *UAS-p35* or *w*; *UAS-lacZ*) transgenic males. Ten female progeny of each genotype were examined.

Brain Dissection

For each dissection, a specimen is placed in 70% ethanol in a 1.5 ml centrifuge tube. After one minute in ethanol, the fly is placed in Ringer's solution and the wings and legs are removed. Using one set of forceps to pinch the proboscis, a small section of the back of the head containing no brain tissue is grasped. Next, the set of forceps that had been previously holding the proboscis are used to pinch an area at the back of the head adjacent to the other set of forceps to produce a small tear by pulling the forceps away from each other. By pinching the proboscis, one set of forceps is then used to remove the cuticle on one side of the back of the head as well as the cuticle surrounding the eye and optic lobe. Once this is accomplished, one set of forceps is positioned such that it holds the remaining posterior head cuticle, while the other set removes the proboscis and other mouthparts. Finally, the remaining sections of cuticle are removed, including the antennae, the remaining eye cuticle and the underside of the head, exposing the brain fully and intact.

Acridine Orange Staining

Acridine orange is a vital dye that specifically labels cells undergoing apoptosis in *Drosophila melanogaster*. It has been shown to be specific for apoptotic cells and will not label the chromatin of cells dying by oxygen starvation or necrosis (Abrams *et al.*, 1993). When acridine orange is used, increased levels of apoptosis are reflected by increased fluorescence. This allows one to compare apoptosis in the brains of flies of different genotypes. Please note that the freshly made 5 µg/ml acridine orange (Sigma, MO) stain is stored in a dark container at 4°C (Bonini, 2000).

Once isolated, the brain is transferred from the Ringer's solution onto a slide with a P1000 micropipette tip along with ~20 µl of Ringer's solution. The Ringer's solution is removed from the slide and replaced with 30 µl of 5 µg/ml acridine orange. The slide is stained for five minutes, at which time the stain is removed and the specimen rinsed briefly with Ringer's solution. The specimen is immediately viewed through fluorescent optics using a Nikon Eclipse E600 microscope and photographed with a Leica DFC 500 digital camera using the layered Montage technique featured on the Leica Application Suite Program in order to obtain a picture of three different planes of view of the specimen. For each genotype examined, ten specimens were photographed and analyzed in this experiment.

Apoptotic Analysis

When stained with acridine orange, cells undergoing apoptosis exhibit bright fluorescence under fluorescent microscopy. The image analysis program ImageJ (available online at <http://rsb.info.nih.gov/ij/>) was used to analyze the greyscale values for each specimen once pictures had been taken of each specimen in a genotype. A more intensely fluorescent specimen would possess a higher average greyscale value than would a less intensely fluorescing specimen. The image of each specimen was viewed using the ImageJ program and the contours of each specimen were traced (ImageJ Area Calculator available online at <http://rsb.info.nih.gov/ij/plugins/area.html>). The statistical software Minitab was used to analyze the greyscale data obtained through ImageJ. The p-values were obtained by conducting post-hoc contrast tests using SAS statistical software.

Example of Analysis

In this study, freshly dissected female adult fly brains expressing the dopaminergic neuronal transgene, *tyrosine hydroxylase-GAL4* (*TH-GAL4*; Friggi-Grelin *et al.*, 2003) were examined for cell death (Table 1). Through breeding, the *TH-GAL4* transgene was placed in combination with two different responsive genes (*p35* and *lacZ*) fused downstream of copies of the *GAL4*-responsive upstream activation sequence (*UAS*). The *p35* gene is an anti-apoptotic baculovirus gene that can suppress the effects of cell death in *Drosophila melanogaster* (Hay *et al.*, 1994). The *lacZ* gene was used as a control gene as it should have neither increased nor prevented *GAL4*-induced apoptosis.

Table 1. Comparison of fluorescence in brains stained with acridine orange (5 mg/mL) for four genotypes of adult *Drosophila* brains.

Genotype	Sample Size	Mean Greyscale	Standard error
Control (progeny of <i>OrR</i> females crossed to <i>w</i> ¹¹¹⁸ males)	10	36.7924	3.1791
<i>w</i> ; <i>TH-GAL4/TH-GAL4</i>	10	51.6683	3.8982
<i>w</i> ; <i>TH-GAL4/UAS-lacZ</i>	10	51.6948	3.4347
<i>w</i> ; <i>TH-GAL4/UAS-p35</i>	10	36.4599	4.4692

Table 2. Contrast test results for three genotype comparisons for levels of apoptosis in the brain.

Test Comparison	Degrees of freedom (DF)	Contrast sums of squares (CS)	Mean sums of squares (MS)	F-statistic	p-value
Control vs. <i>w</i> ; <i>TH-GAL4/TH-GAL4</i>	1	1106.462004	1106.462004	7.75	0.0085
<i>w</i> ; <i>TH-GAL4/TH-GAL4</i> vs. <i>w</i> ; <i>TH-GAL4/UAS-lacZ</i>	1	0.003511	0.003511	0.00	0.9961
<i>w</i> ; <i>TH-GAL4/UAS-lacZ</i> vs. <i>w</i> ; <i>TH-GAL4/UAS-p35</i>	1	1160.510890	1160.510890	8.13	0.0072

In our sample statistical analysis (Table 2), i) *TH-GAL4* homozygous flies were compared to the controls that do not express *GAL4*; ii) *TH-GAL4* homozygotes were compared to flies possessing one copy of the *TH-GAL4* gene and one copy of the *UAS-lacZ* gene; and iii) *TH-GAL4* flies co-expressing *lacZ* were compared to *TH-GAL4* flies co-expressing *p35*. The tolerance of Type I error (α) was initially set at 5%; however, the comparisons of genotypes in this study lack independence (data not shown), therefore decisions based on rejection at $\alpha = 0.05$ may be inaccurate. As a result, it

is statistically necessary to apply a more conservative approach and the tolerance of type I error must be reduced. This is accomplished by performing a Dunn-Sidak re-adjustment using the following formula:

$$\alpha' = 1 - (1 - \alpha)^{1/k}$$

where α' represents the adjusted tolerance of Type I error, α represents the original tolerance of Type I error and k represents the number of test comparisons present in the contrast test table (Sokal and Rohlf, 1995). In this case, the adjusted α' was determined to be 0.0170.

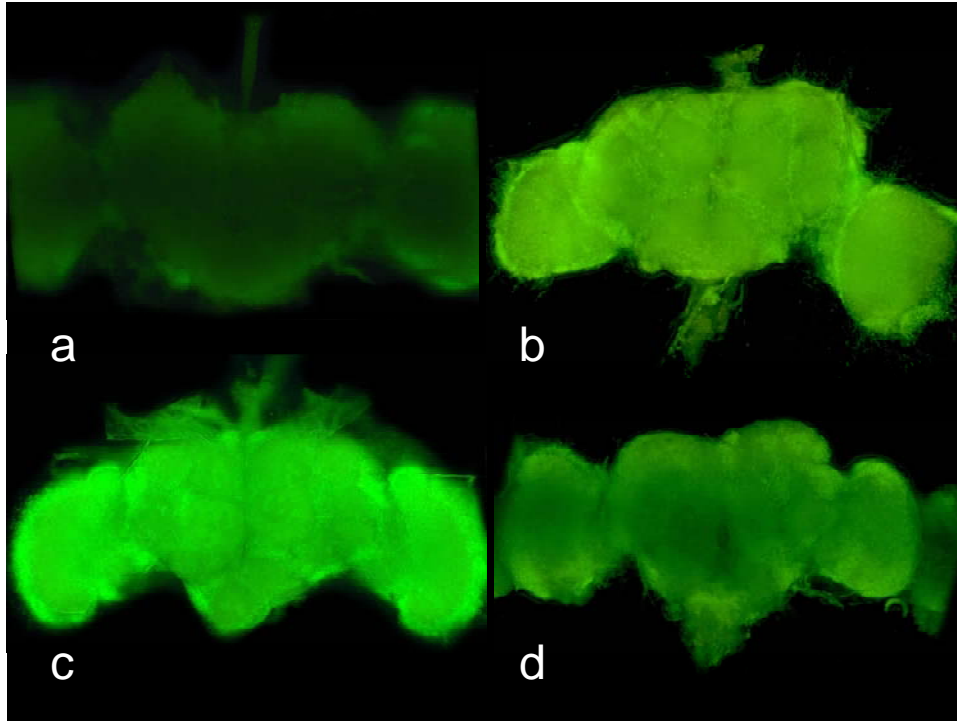


Figure 1. Acridine orange-stained adult brains of a) a control (the progeny of *OrR* females and *w¹¹¹⁸* males); b) *w; TH-GAL4*; c) *w; TH-GAL4/UAS-lacZ*; and d) *w; TH-GAL4/UAS-p35*.

In comparison to the non-*GAL4* control with an average greyscale value and standard error of 36.7924 ± 3.1791 , the *w; TH-GAL4* brains exhibited higher levels of staining as indicated by the elevated average greyscale value and standard error (51.6683 ± 3.8982). In order to determine if a significant difference between the fluorescence levels in the control and in the *TH-GAL4* homozygotes existed, a contrast test was conducted. The p-value was 0.0085; this suggests a significant increase in apoptosis in the brains of the *TH-GAL4* homozygotes when compared to the controls.

Similar mean greyscale values and standard errors were obtained for *w; TH-GAL4* (51.6683 ± 3.8982) and *w; TH-GAL4/UAS-lacZ* (51.6948 ± 3.4347) brains. A contrast test was conducted in order to determine if there existed a significant difference between the fluorescence levels of both groups of brains. There is no significant difference in the amount of apoptosis in the brains of these two genotypes of flies (p-value = 0.9961). This suggests that *TH-GAL4*-induced apoptosis may not increase in a dosage-dependent manner.